BRAIN
A JOURNAL OF NEUROLOGY

Progressive gait ataxia following deep brain stimulation for essential tremor: adverse effect or lack of efficacy?

Martin M. Reich,[1*] Joachim Brumberg,[2,*] Nicolò G. Pozzi,[1] Giorgio Marotta,[3] Jonas Roothans,[4] Mattias Åström,[4,5] Thomas Musacchio,[1] Leonardo Lopiano,[6] Michele Lanotte,[6] Ralph Lehrke,[7] Andreas K. Buck,[2] Jens Volkmann[1] and Ioannis U. Isaias[1]

*These authors contributed equally to this work.

Thalamic deep brain stimulation is a mainstay treatment for severe and drug-refractory essential tremor, but postoperative management may be complicated in some patients by a progressive cerebellar syndrome including gait ataxia, dysmetria, worsening of intention tremor and dysarthria. Typically, this syndrome manifests several months after an initially effective therapy and necessitates frequent adjustments in stimulation parameters. There is an ongoing debate as to whether progressive ataxia reflects a delayed therapeutic failure due to disease progression or an adverse effect related to repeated increases of stimulation intensity. In this study we used a multimodal approach comparing clinical stimulation responses, modelling of volume of tissue activated and metabolic brain maps in essential tremor patients with and without progressive ataxia to disentangle a disease-related from a stimulation-induced aetiology. Ten subjects with stable and effective bilateral thalamic stimulation were stratified according to the presence (five subjects) of severe chronic-progressive gait ataxia. We quantified stimulated brain areas and identified the stimulation-induced brain metabolic changes by multiple ^{18}F-fluorodeoxyglucose positron emission tomography performed with and without active neurostimulation. Three days after deactivating thalamic stimulation and following an initial rebound of symptom severity, gait ataxia had dramatically improved in all affected patients, while tremor had worsened to the presurgical severity, thus indicating a stimulation rather than disease-related phenomenon. Models of the volume of tissue activated revealed a more ventrocaudal stimulation in the (sub)thalamic area of patients with progressive gait ataxia. Metabolic maps of both patient groups differed by an increased glucose uptake in the cerebellar nodule of patients with gait ataxia. Our data suggest that chronic progressive gait ataxia in essential tremor is a reversible cerebellar syndrome caused by a maladaptive response to neurostimulation of the (sub)thalamic area. The metabolic signature of progressive gait ataxia is an activation of the cerebellar nodule, which may be caused by inadvertent current spread and antidromic stimulation of a cerebellar outflow pathway originating in the vermis. An anatomical candidate could be the ascending limb of the uncinate tract in the subthalamic area. Adjustments in programming and precise placement of the electrode may prevent this adverse effect and help fine-tuning deep brain stimulation to ameliorate tremor without negative cerebellar signs.

1 Department of Neurology, University Hospital and Julius-Maximilian-University, Wuerzburg, Germany
2 Department of Nuclear Medicine, University Hospital and Julius-Maximilian-University, Wuerzburg, Germany
3 Department of Nuclear Medicine, Fondazione IRCCS Ca' Granda – Ospedale Maggiore Policlinico, Milano, Italy
4 Medtronic Neuromodulation, Medtronic Eindhoven Design Center, The Netherlands
5 Department of Biomedical Engineering, Linköping University, Sweden
6 Neuroscience Department, University of Turin Medical School, Turin, Italy
7 Department of Stereotactic Neurosurgery, St. Barbara – Klinik, Hamm, Germany

Correspondence to: Prof. Dr. Jens Volkmann, University Hospital Wuerzburg,
Department of Neurology,
Josef-Schneider-Str.11, D-97080 Wuerzburg, Germany
E-mail: Volkmann_J@ukw.de

Introduction

Motor disability in essential tremor results predominantly from the complex interaction of postural-, action- and intention-tremor with goal-directed hand movements, but ~10–15% of patients additionally present mild cerebellar symptoms, such as saccadic abnormalities (Helmchen et al., 2003), dysmetria or impaired tandem gait (Flament and Hore, 1986; Hallett et al., 1991; Fasano et al., 2010). There is an ongoing debate on whether a cerebellar dysfunction in essential tremor is caused by disease progression and neurodegeneration (Louis et al., 2007) or a functional disruption of the cerebello-thalamo-cortical network through the interference of tremor-related neuronal oscillations with normal cerebellar timing function (Solomon et al., 1994; Elble, 1998; Deuschl et al., 2000; Blangero et al., 2009; Elble, 2009).

A strong argument in favour of a cerebellar dysfunction stems from the observed effects of deep brain stimulation (DBS) of the (sub)thalamic area. Fasano et al. (2010) described a parallel improvement of tremor and disease-related gait ataxia in essential tremor with moderate stimulation amplitudes, while a further increase of stimulation intensity (supra-therapeutic) led to recurrence of gait and balance problems, despite tremor remaining suppressed. Similar divergent effects have been observed for tremor and dysmetria during reach-to-grasp movements (Groppa et al., 2014). These findings have pointed to two segregated cerebellar networks being modulated by DBS, a circuit for the combined control of tremor and disease-related ataxia and a second circuit inducing ataxia by supra-therapeutic stimulation (Herzog et al., 2007; Groppa et al., 2014).

Thalamic DBS is now considered a mainstay treatment for disabling and drug-refractory essential tremor (Putzke et al., 2004; Pahwa et al., 2006; Fasano et al., 2010). The procedure has a high responder rate and efficacy (beyond 10 years) for severe tremors and further improved by moving the stimulation target from the ventro-intermediate thalamic nucleus to subthalamic fibre pathways (Herzog et al., 2007; Blomstedt et al., 2009; Baizabal-Carvallo et al., 2014; Coenen et al., 2014). However, there are also reports about delayed failure of DBS. A typical clinical scenario is an improvement of tremor after initial programming, but a subsequent decline in efficacy and the need for repeated stimulation adjustments. In these cases, progressive motor disability results from a worsening of intention tremor rather than action or postural tremor and the emergence of additional cerebellar symptoms, such as truncal ataxia and unsteady gait. Often these patients suffer also from tremor rebound, an acute exacerbation of tremor and ataxia beyond the presurgical baseline when turning the stimulation off. Several explanations have been proposed, including tolerance development, misdiagnosis, lead misplacement and disease progression. The exact proportion of essential tremor patients with delayed DBS failure is unknown, but a recent single centre study described a rate of 25% among 28 patients (Favilla et al., 2012). After an extensive work-up, the authors concluded that only one of seven patients with DBS failure fulfilled their criteria for tolerance, whereas the others likely suffered from disease progression (Favilla et al., 2012). Interestingly, it was not addressed in this study, whether the severe cerebellar syndrome could be an adverse effect of prolonged DBS, given the fact that supra-threshold stimulation provokes ataxia and that rescue programming attempts often lead to increasing stimulation intensity.

Following the hypothesis of a stimulation-induced (rather than disease-related) aetiology, we compared the clinical outcome of DBS, the disease severity after prolonged stimulation wash-out, the volume of tissue activated (VTA) and the DBS-related cerebral metabolic changes [^{18}F-fluorodeoxyglucose (FDG) PET] in essential tremor patients with and without DBS failure.

Materials and methods

Subjects and clinical test battery

This study involved 10 patients with pharmacologically intractable essential tremor and bilateral DBS of the (sub)thalamic area. Entry criteria were the diagnosis of essential tremor according to the Tremor Investigation Group and the Consensus Statement of the Movement Disorder Society Group (Deuschl et al., 1998) and stable clinical response to thalamic stimulation for at least 6 months. Exclusion criteria were any neurological comorbidity (e.g. polyneuropathy). Patients receiving anti-tremor medication at the time of assessment were also excluded. All patients underwent a preoperative 3 T MRI (T$_1$, T$_2$, T$_2$*, FLAIR, Trio, Siemens Medical Systems) to rule out morphological anomalies.

We recruited five patients with a secondary DBS failure characterized mainly by chronic-progressive gait ataxia (ET$_{ataxia}$:

two males; age 75 ± 5 years; disease duration 25 ± 10 years; time from electrode implantation 23 ± 7 months; average $\pm$ standard error of the mean). After an initial benefit on tremor without any side effect (e.g. gait difficulties), these patients showed a progressive decline in DBS efficacy (starting >3 months after initial programming) and needed repeated stimulation adjustments to compensate for the reduced tremor control. Subsequently, they developed a chronic-progressive gait ataxia (in the absence of any other DBS-related adverse event) over a period of at least 4 weeks of chronic stimulation with unchanged settings.

We also recruited five patients without any gait difficulties or unsteadiness matched for age, disease duration, time from surgery ($ET_{control}$: three males; age 54 ± 14 years; disease duration 31 ± 11 years; time from electrode implantation 25 ± 7 months). The Fahn-Tolosa-Marin Tremor Rating Scale (TRS) and the Scale of the Assessment and Rating of Ataxia (SARA) were performed. We recorded only SARA item 1 to 3 ($SARA_{1-3}$) as referring to axial signs and not affected by upper limb tremor.

Patients were assessed in the following three conditions: (i) stimulation on (stim-ON) with the clinically optimized and chronically used stimulation parameters; (ii) immediately after deactivating the stimulation ($stim-OFF_{direct}$); and (iii) stimulation off for 72 h ($stim-OFF_{72h}$). Of note, 72 h was the minimum time interval after which all subjects reported an improvement of gait difficulties.

The stimulation parameters were controlled by a physician independently from this study and provided a sustained improvement of tremor without any acute side effect. Parameters remained unchanged for at least 4 weeks prior to the study.

Standard protocol approvals, registrations and patient consents

The study was approved by the institutional review board of the University Hospital of Wuerzburg and by the Governmental Radiation Protection Authority (Bundesamt für Strahlenschutz, Aktenzeichen: Z5-22463/2-2015-010). Written informed consent was obtained from all subjects.

Surgical procedure

The surgical procedure has been previously described in detail (Hamel *et al.*, 2002; Herzog *et al.*, 2007). In the present study, all subjects received quadripolar macroelectrodes (model 3389, Medtronic Inc.). The stereotactic coordinates of each contact of the quadripolar macroelectrode related to the midpoint of the line between anterior and posterior commissure were calculated based on fusion of the preoperative stereotactic and postoperative MRI. The mean coordinates of the active contacts were x: 12.55 ± 1.63 mm, y: -5.15 ± 1.44 mm, z: -0.85 ± 1.60 mm in ET_{ataxia} and x: 12.09 ± 1.62 mm, y: -4.55 ± 1.19 mm, z: 0.29 ± 2.10 mm in $ET_{control}$.

Volume of tissue activated modelling

Correct lead positioning was verified with SureTune™ (Medtronic Eindhoven Design Center, MEDC) by fusing the preoperative stereotactic MRI with a postoperative CT performed more than 40 days after electrode implantation. To visually compare lead location as well as site of stimulation between ET_{ataxia} and $ET_{control}$, patient images were registered to a common probabilistic anatomy model of the ventral thalamus and subthalamic area. This probabilistic anatomy model was created by registration and normalization of 50 preoperative T_2-weighted MRI volumes. Registration was carried out with a rigid registration algorithm based on normalized gradient fields (Rühaak *et al.*, 2015), together with a local bounding box of $30 \times 30 \times 30$ mm^3 applied around the target area to define the volume used for registration. VTAs were simulated and displayed for each lead based on the applied stimulation parameters (Table 1) (Astrom *et al.*, 2014). A mean VTA was created for each cohort by aggregating all VTAs of a single group, and allegorize only voxels that overlapped by $\geqslant 2$ VTAs. Volume of mass and centre of mass were calculated for each mean VTA. In addition, the overlapping volume of the mean VTAs of the two patient groups was calculated.

Imaging technique and PET data analysis

PET scans were performed with the PET/CT scanner Biograph mCT 64 (Siemens Medical Solutions) at the University Hospital of Wuerzburg.

The patients were scanned on 2 days. On the first day scanning was conducted with the stim-ON, with chronically used settings. A second scan was performed after 72 h stimulation off ($stim-OFF_{72h}$). The PET study was started 30 min after the injection of 208 ± 16.5 MBq of FDG. Before each PET session, patients fasted overnight. The studies were performed with the subjects' eyes open in a dimly lit room and with minimal auditory stimulation. The patients' clinical condition was monitored by a neurologist (I.U.I.) from the injection of the radioligand until the end of the scan, and no patient had overt tremor or ataxia as a potential confounder of cerebral FDG uptake.

PET was performed in 3D mode for 10 min/one bed position using a 400×400 matrix with an axial resolution of 2 mm full-width at half-maximum and an in-plane resolution of 4.7 mm. CT scans for attenuation correction were acquired using a low-dose protocol. PET data were reconstructed iteratively (24 subsets, three iterations, Gaussian filtering) using HD reconstruction mode.

A group of 10 age- and gender-matched healthy subjects (HC; five males; age 62 ± 14 years), previously acquired with the same methods, served as control group.

FDG data preprocessing was performed with statistical parametric mapping (SPM 8, Wellcome Department of Cognitive Neurology, University College, London). Scans were spatially normalized to a FDG PET template in the standardized Montreal Neurological Institute (MNI) space (16 iterations, non-linear transformation and trilinear interpolation) and then smoothed using a Gaussian kernel at full-width at half-maximum = 8 mm. Paired *t*-tests were used to assess stimulation effect in voxel-wise maps. Voxel-wise comparisons between patients with essential tremor and healthy subjects were performed using the flexible factorial model. The SPM maps were obtained at a height threshold of $P < 0.005$, cluster extent $k \geqslant 30$ voxels. We considered significant peak levels with Z score $\geqslant 3.0$.

Table 1 Chronic stimulation parameters

Subjects	IPG	Stimulation parameters							
		Right contact	Right (mA)	Right (µs)	Right (Hz)	Left contact	Left (mA)	Left (µs)	Left (Hz)
ETataxia_01	Medtronic Activa PC	1 + 0−	1.8	60	180	9 + 8−	2.3	60	180
ETataxia_02	Medtronic Activa PC	G + 8−	2.0	60	125	3 + 0−	3.0	60	125
		interleaved	interleaved			interleaved	interleaved		
		G + 9−	1.5			3 + 1−	3.0		
ETataxia_03	Medtronic Activa PC	10 + 9−8−	3.3	60	180	2 + 1−0−	3.9	60	180
ETataxia_04	Medtronic Activa PC	G + 1−	2.1	60	180	G + 8−	1.7	60	180
ETataxia_05	St. Jude Brio	3 + 4−	3.5	50	160	3 + 2−	3.0	50	160
Mean			2.49	58	165		2.78	58	165
ETcontrol_01	Medtronic Activa PC	G + 2−	3.0	60	180	G + 8−	1.7	60	180
ETcontrol_02	Medtronic Activa PC	G + 8−	0.9	60	140	G + 0−	1.2	60	140
ETcontrol_03	Medtronic Activa PC	10 + 9−	0.9	90	130	G + 1−	2.5	60	130
ETcontrol_04	Medtronic Activa PC	G + 1−	2.3	90	130	G + 9−	2.0	60	130
ETcontrol_05	Medtronic Activa PC	G + 10−	2.0	60	170	G + 1−	2.6	60	170
Mean			1.82	72	150		2.0	60	150

IPG = implantable pulse generator.

SPM findings were also confirmed by a *post hoc* volume of interest analysis. We calculated global and regional cerebral metabolic rates for glucose consumption within the SPM predefined brain areas. To reduce intersubject variability, the regional metabolic measurements were normalized by global values.

Statistical analysis

Statistical analyses were performed with the JMP statistical package, (version 12, SAS Institute, Inc., Cary, NC, USA). Gender difference between groups was analysed using Pearson's chi-squared test. Other differences between groups were analysed by means of Mann-Whitney U-test. The threshold level of statistical significance was set at $P < 0.05$.

Results

Clinical evaluation

Evaluation of the TRS demonstrated a significant tremor reduction ($>70\%$) during stim-ON in all patients. $ET_{control}$ showed greater benefit from stimulation (TRS scores for $ET_{control}$ 2.0 ± 2.3 and ET_{ataxia}: 7.8 ± 4.2, $P = 0.014$). The mean TRS score in stim-OFF$_{72h}$ was similar between the two groups of patients (ET_{ataxia}: 17.2 ± 5.9 and $ET_{control}$: 14.2 ± 2.3, $P = 0.34$). Age, disease duration and time after implantation did not influence tremor improvement.

As expected, the SARA$_{1-3}$ score in stim-ON was significantly higher for ET_{ataxia} than $ET_{control}$ (6.2 ± 0.6 versus 0.2 ± 0.6, $P = 0.001$).

Directly after switching off the stimulation (stim-OFF$_{direct}$), we observed a severe rebound of ataxia in both groups, sometimes leaving the patient bedridden, which gradually disappeared in the follow-up period.

After 72 h of deactivated stimulation (stim-OFF$_{72h}$), all ET_{ataxia} subjects reported a significant improvement in gait difficulties and unsteadiness, which was mirrored by a lower SARA$_{1-3}$ score (Fig. 1).

Volume of tissue activated by high-frequency stimulation

Mean VTA volumes of the ET_{ataxia} and $ET_{control}$ group were 86 mm^3 and 68 mm^3, respectively, with an overlap of the two volumes by 37.5 mm^3. Mean VTA of ET_{ataxia} was located inferior and posterior in relation to mean VTA of $ET_{control}$ centre of mass mean VTA reflecting this finding (ET_{ataxia}: x: 11.6 mm; y: 4.7 mm; z: 1.0 mm; $ET_{control}$: x: 13.1 mm; y: 4.2 mm, z: 2.2 mm) (Fig. 2A).

Brain metabolic changes induced by brain stimulation

Pairwise correlations of stimulation-induced changes are presented in Table 2 and Fig. 3. The most prominent effect of stimulation was a distinctive increment of FDG uptake in the cerebellar nodule of ET_{ataxia} patients but not in $ET_{controls}$. DBS also had a marked impact on thalamic metabolic activity of both essential tremor cohorts, as seen by the increased FDG uptake in the left and right thalamic ventral posterior nucleus (which corresponds to the ventral intermedius nucleus) (Nazzaro *et al.*, 2013). Similar results were found when evaluating glucose consumption of predefined volume of interest. Of relevance, no difference was found when comparing cerebellar glucose consumption of all essential tremor (in stim-OFF$_{72h}$) to healthy controls, which was also true when considering only the volume of interest placed on the cerebellar nodule.
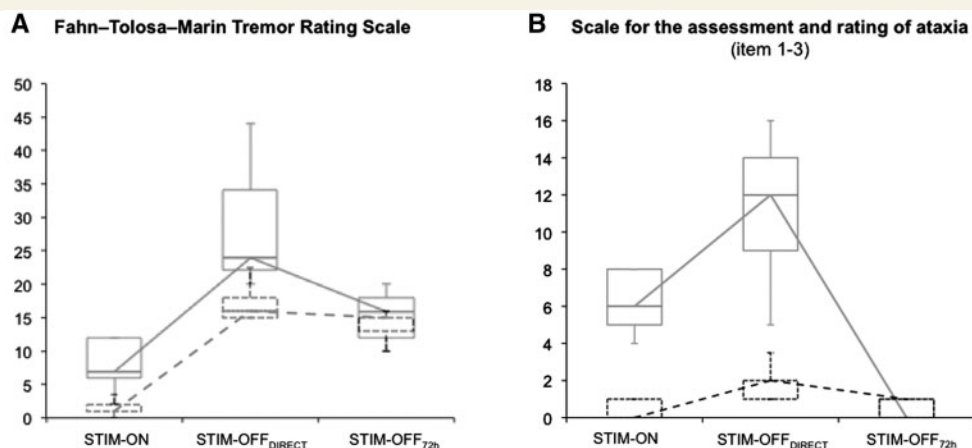
Figure 1 Clinical outcomes. (**A**) Fahn-Tolosa-Marin Tremor Rating Scale and (**B**) Assessment and Rating of Ataxia (mean ± SD) item 1–3 under chronic thalamic stimulation (stim-ON), directly after deactivating DBS (stim-OFF$_{direct}$) and after stimulation off for 72 h (stim-OFF$_{72h}$). Tremor greatly ameliorated ($> 70\%$) in all patients after thalamic stimulation. We observed a severe rebound of tremor and ataxia directly after switching off the stimulation (stim-OFF$_{direct}$), which disappeared in the follow-up period (stim-OFF$_{72h}$). ET$_{control}$ = dotted line; ET$_{ataxia}$ = continuous line.

Discussion

In this study, we forward evidence that chronic-progressive gait ataxia in subjects with essential tremor is reversible after a prolonged DBS washout and emerges from a stimulation-induced vestibulocerebellar network dysfunction.

Two main observations support this view: (i) a gradual improvement of gait ataxia after pausing stimulation for 72 h; and (ii) increased neuronal metabolic activity in the cerebellar nodule of patients with chronic-progressive gait ataxia as compared to essential tremor without. We further propose that cerebellar dysfunction in subjects with ET$_{ataxia}$ is a remote effect of inadvertent antidromic stimulation of vestibulocerebellar-thalamic afferents within the subthalamic target area of DBS.

Several studies have reported cerebellar ataxia as a clinical feature of advanced essential tremor (Fasano *et al.*, 2010). However, it is worth noting that the chronic-progressive gait ataxia described here clearly differs from the disease-related ataxia, which is milder in its presentation and is typically ameliorated by thalamic-stimulation, irrespective of the affected body site and independently of co-existing tremor. Of note, a sufficiently long washout of DBS is required to overcome the initial tremor and ataxia rebound and re-establish a disease baseline, which may explain the partially conflicting observations in previous studies. A previous study reported a worsening of untreated tremor 1 year after DBS implantation, but thalamic stimulation was deactivated for 30 min only. As shown by our results (Fig. 1), clinical changes after such a small time interval possibly reflect just the pausing of stimulation *per se* rather than the progression of the disease.

It is worth noting that chronic-progressive gait ataxia also differs from acute upper limb ataxia induced by (supra)therapeutic stimulation (Groppa *et al.*, 2014). The delayed onset of gait ataxia with chronic DBS suggests a maladaptive component probably involving a different cerebello-thalamo-cortical fibre system. Alternatively, intracerebellar compensatory mechanisms may be taken into account. Indeed, the lateral hemispheres of the cerebellum can greatly compensate for the loss of function of the vermis and the flocculonodular lobe, as seen for example in subjects with Joubert syndrome (Romani *et al.*, 2013).

Several physiological studies in monkey and humans have provided evidence that the cerebello-thalamo-cortical circuit is essential for gait and balance (Diener *et al.*, 1984; Itō, 1984; Hallett and Massaquoi, 1993; Armstrong and Marple-Horvat, 1996; Cooper *et al.*, 2000; Ilg *et al.*, 2007; Blangero *et al.*, 2009). Real locomotion FDG PET studies have also confirmed a prominent activation in the vermal and paravermal cerebellum, with extensions into the superior cerebellar peduncle bilaterally (Ishii, 1995; la Fougere *et al.*, 2010).

Three distinguished cerebello-thalamo-cortical subcircuits might be particularly relevant in the pathophysiology of thalamic stimulation-induced effects in essential tremor (Fig. 4).

First, the dentato-thalamic tract is the main output of the lateral cerebellum and projects to the motor cortex via the ventrolateral thalamus. The dentato-thalamic system is mainly involved in the control of voluntary movements of the extremities, such as single-joint and multi-joint goal-directed movements (Schwartz *et al.*, 1987; Marple-Horvat *et al.*, 1998; Marple-Horvat and Criado, 1999; Cooper *et al.*, 2000). These fibres are supposed to mediate the tremor and ataxia suppressing effect of thalamic-stimulation in essential tremor (Groppa *et al.*, 2014).

Second, the cerebello-rubrospinal system is involved in the sensory-to-motor transformation required for cerebellar control of goal-directed limbs movements. Stimulation (supratherapeutic) of these fibres was shown to induce the reappearance of ataxia, in particular the spatial variability during the deceleration phase of reach-to-grasp movements,
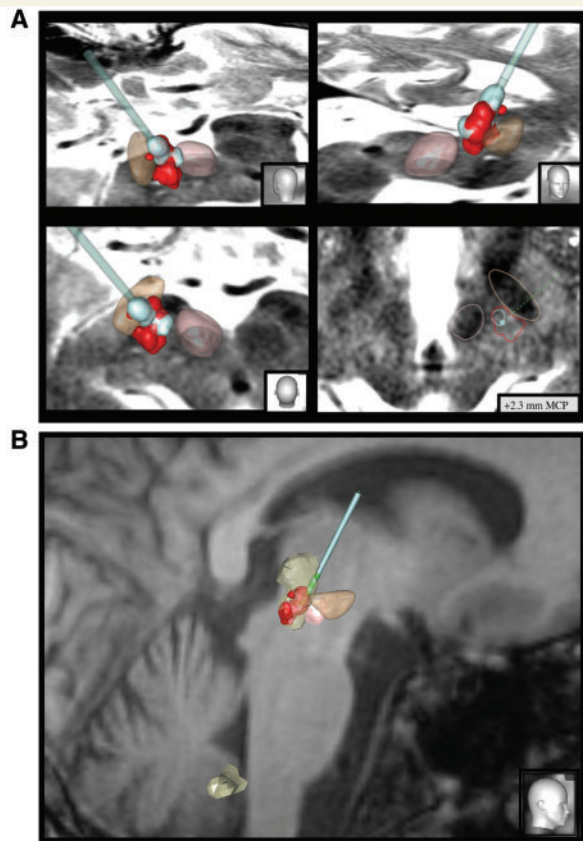
Figure 2 Reconstruction of the mean volume of tissue activated for ET$_{control}$ and ET$_{ataxia}$ on a standard MRI. (A) Mean VTAs (voxels covered by $\geqslant 2$ VTA in the co-registration of each subject) in 3D and axial plane on T$_2$-weighted MRI Space. ET$_{control}$ = 70 mm^3 (light blue volume) and ET$_{ataxia}$ = 90 mm^3 (red volume). In comparison to the mean VTA of ET$_{control}$, the mean VTA of ET$_{ataxia}$ is closer to the posteromedial border of the subthalamic nucleus (light brown) and the risk of ataxic gait increases with greater proximity to the red nucleus (pink). **(B)** Co-registration of volume of tissue activation (VTA) modelling and statistical parametric mapping. Mean VTA of ET$_{ataxia}$ (red) was related to increased metabolic rates for glucose consumption in the cerebellar nodule and electrode surrounding area (light grey) possibly due to antidromic activation of cerebello-thalamic fibres caused by current spreading into the ascending limb of the uncinate tract. Subthalamic nucleus (light brown); red nucleus (pink).

while maintaining near complete suppression of tremor (Groppa *et al.*, 2014).

Third, the fastigio-bulbar tract projects from the cerebellar vermis and nodule to the motor thalamus, spinal cord and vestibular system. In particular, its ascendant uncinate tract projects to the ventrolateral/intralaminar thalamic nuclei (Paxinos and Mai, 2004). This tract is particularly important for axial coordination during movements and its failure results in severe gait ataxia (Sprague and Chambers, 1953; Imperato *et al.*, 1984).

These cerebello-thalamic fibres run parallel with a clear functional-anatomical organization, the appendicular movements control being situated in a lateral bundle and the axial one more medially. In the (sub-)thalamic area however, these fibres run in close vicinity and effective DBS targeting the lateral fibres may inadvertently co-stimulate medial cerebello-thalamic tracts (Groppa *et al.*, 2014). Indeed, our study showed that the VTA of ET$_{ataxia}$ is located more posteromedial and caudally in the (sub)thalamic area when compared to ET$_{control}$.

VTA modelling is a novel tool that computes the region in which certain stimulation settings may induce action potentials in model neurons (Butson *et al.*, 2011). Current VTA modelling depends on stimulation parameters, tissue impedance and tissue anisotropy (McNeal, 1976; Butson *et al.*, 2006). A possible limitation of this model is the dependency on *a priori* assumptions about the membrane properties of the stimulated axons. However, it was recently shown that VTA mirrored such neuronal proprieties as clinically defined (i.e. chronaxies) (Reich *et al.*, 2015). Finally, VTA assumes that the primary effect of DBS is to activate myelinated axons, which was proved by several studies (Holsheimer *et al.*, 2000; Paxinos and Mai, 2004; Groppa *et al.*, 2014).

Current spreading into the ascending limb of the uncinate tract may directly influence the activity of cerebellar nodule as suggested by an increased FDG uptake in this area. Indeed, it was shown that DBS stimulation could affect functionally connected brain areas remote from the stimulation site (Hilker *et al.*, 2008). Accordingly, we advance the hypothesis that the hypermetabolism in the cerebellar

Table 2 Brain areas (coordinates and regions in Talairach space) with significantly increased glucose consumption

P	k	Region	Coordinates (mm)			Z-score
			x	y	z	
ET$_{ataxia}$						
Stim-ON versus stim-OFF$_{72h}$						
0.000	37	Thalamus, VP (left)	−14	−18	0	3.84
0.000	31	Cerebellum, nodule	4	−50	−34	3.55
0.001	66	Thalamus, VP (right)	22	−18	6	3.12
ET$_{control}$						
Stim-ON versus stim-OFF$_{72h}$						
0.000	43	Thalamus, VP (right)	18	−20	−2	3.75

Nucleus ventralis posterior (VP) corresponds to the ventral intermedius nucleus in the stereotactic atlas of Schaltenbrand and Wahren (Nazzaro *et al.*, 2013).
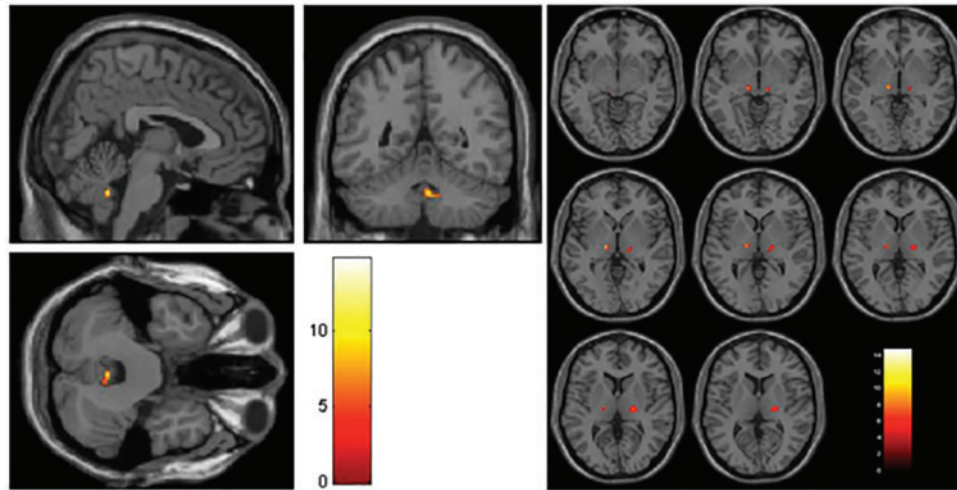
Figure 3 SPM analysis of ET$_{ataxia}$ in stim-ON versus stim-OFF$_{72h}$. Chronic stimulation compared to a 72 h stimulation washout is associated with significant increases of FDG in the cerebellar nodule and both thalamic ventral intermedius nucleus in the ET$_{ataxia}$ group.
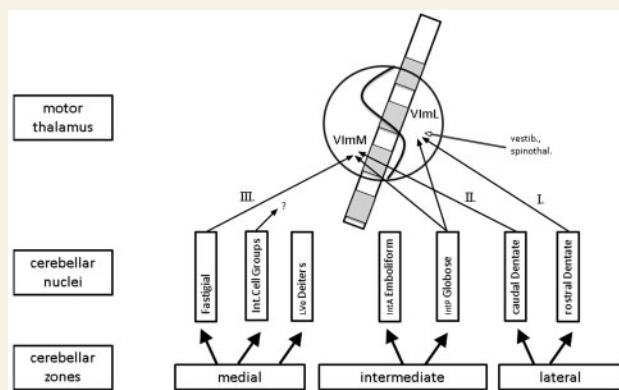

Figure 4 Modified diagram of parallel channels in the cerebello-thalamic-cortical projection from Paxinos and Mai (2004). This model shows the subdivision of the cerebellar territory of the motor thalamus (ventral intermedius nucleus) into ventrolateral (VImL) and dorsomedial subparts (VImM). The overlap of vestibular and spino-thalamic projections in the VImL is indicated. It also shows the connections of the cerebellar nuclei with the thalamus. **(I)** The dentato-thalamic tract, arising from the lateral cerebellar zones, is the presumed target of effective thalamic DBS. **(II)** The rubro-olive-cerebellar tract, which originates from olivary nucleus to be distributed to the cerebellar hemisphere via raphe nucleus. It might be causative of the (supratherapeutic) stimulation-induced limb ataxia. **(III)** The ascendant uncinate tract (fastigulus bulbar fibres) that arises from the medial cerebellar structures and it is probably associated with chronic-progressive gait ataxia. The stimulation lead shows the 'classical' surgical target: the second lowest electrode in the middle of the VIim and the lowest electrode on the border to the white matter (posterior zona incerta).

nodule shown in ET$_{ataxia}$ is due to antidromic activation of cerebello-thalamic fibres caused by the stimulation electric field. A cerebellar compensatory activity due to tremor seems unlikely as we tested the patients in resting condition, closely monitoring the complete absence of upper limb movements that could affect FDG uptake. Moreover, an antidromic activation of dentate-thalamic fibres—the presumed target of effective thalamic DBS—can also be excluded, as it would induce metabolic changes of the lateral cerebellum. Here, we also confirm a previous study reporting no abnormalities of glucose metabolism in the cerebellum of non-DBS treated essential tremor patients. These findings further support a stimulation-induced hypermetabolism rather than a disease-related cerebellar pathology (Hallett and Dubinsky, 1993; Song *et al.*, 2015). We also confirmed previous reports of an enhanced neuronal activity in the area surrounding the active electrodes (i.e. thalamic area) of all essential tremor subjects (Hilker *et al.*, 2008; Martin-Blanco *et al.*, 2015) and no other brain region.

FDG is a marker of hexokinase activity that regulates the regional cerebral glucose metabolic rate. Quantification of the regional glucose accumulation can be performed by PET and correlates with regional synaptic activity (Otte and Halsband, 2006). In particular, sequential FDG PET is an established method to identify metabolic changes in subcortical structures with comparable size (Hilker *et al.*, 2008; Le Jeune *et al.*, 2009; Wang *et al.*, 2010). Despite being small, the regions of interest (e.g. cerebellar nodule) more than double the resolution of our PET/CT. Partial volume effect is therefore unlikely to occur and even if present, it would underestimate the activity of small structures (Heiss *et al.*, 2004).

A possible limitation of this study is the small sample size. However, the hypermetabolism in the cerebellar nodule was consistently detected in all ET$_{ataxia}$ subjects and the number of included patients is comparable to previous studies addressing a similar topic (Groppa *et al.*, 2014).

In conclusion, our study suggests that chronic-progressive gait ataxia in essential tremor is a reversible cerebellar symptom probably induced by inadvertent stimulation of the
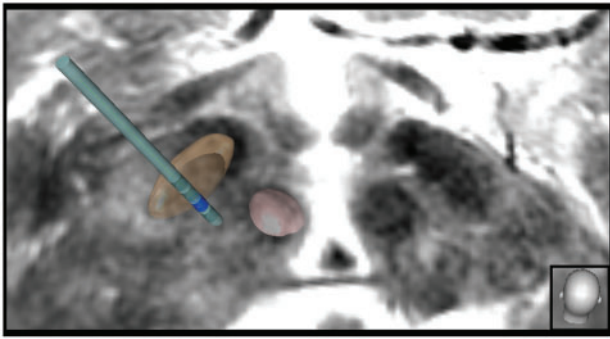
Figure 5 Simulation of an ideal lead placement estimated from the VTA of patients without ataxia. The location corresponds to the posterior subthalamic area as described previously (Velasco *et al.*, 1972; Blomstedt *et al.*, 2009). As depicted on the T_2-weighted MRI the axial targeting plane should be on the level of the maximal diameter of the red nuclei. The lead should be positioned adjacent to the medial border of the subthalamic nucleus, in its posterior third. Therefore, the T_2-weighted hypointense outline of the subthalamic nucleus and of the red nucleus may be used as anatomical references for direct anatomical targeting or verification of stereotactic planning.

ascending limb of the uncinate tract, which in turn affects the cerebellar nodule functioning (Fig. 2B). Following this hypothesis, avoiding a too caudal and ventral placement of standard DBS electrodes or directing current away from this region with novel DBS systems capable of horizontal current steering might prevent this chronic side effect. As estimated from the VTA of patients without ataxia, a relatively safe target to be further refined by intraoperative stimulation results could be the lateral part of the posterior subthalamic area, which has been proposed more than 30 years ago (Velasco *et al.*, 1972) as the optimal target for severe tremors. For direct anatomical targeting on axial T_2-weighted MRI the posterior and medial border of the subthalamic nucleus at the level of the largest diameter of the red nucleus may be used as a reference (Blomstedt *et al.*, 2009) (Fig. 5). As previously suggested, a shorter pulse duration of $< 60\,\mu s$ could constitute an alternative approach of selectively stimulating dentato-thalamic fibres close to the DBS lead based on divergent chronaxies of different subthalamic fibre tracts (Reich *et al.*, 2015).

Funding

Conflicts of interest

Supplementary material

Supplementary material is available at *Brain* online.

References

Armstrong DM, Marple-Horvat DE. Role of the cerebellum and motor cortex in the regulation of visually controlled locomotion. Can J Physiol Pharmacol 1996; 74: 443–55.

Astrom M, Diczfalusy E, Martens H, Wardell K. Relationship between neural activation and electric field distribution during deep brain stimulation. IEEE Trans Biomed Eng 2014; 62: 664–72.

Baizabal-Carvallo JF, Kagnoff MN, Jimenez-Shahed J, Fekete R, Jankovic J. The safety and efficacy of thalamic deep brain stimulation in essential tremor: 10 years and beyond. J Neurol Neurosurg Psychiatry 2014; 85: 567–72.

Blangero A, Menz MM, McNamara A, Binkofski F. Parietal modules for reaching. Neuropsychologia 2009; 47: 1500–7.

Blomstedt P, Fytagoridis A, Tisch S. Deep brain stimulation of the posterior subthalamic area in the treatment of tremor. Acta Neurochir 2009; 151: 31–6.

Butson CR, Cooper SE, Henderson JM, Wolgamuth B, McIntyre CC. Probabilistic analysis of activation volumes generated during deep brain stimulation. Neuroimage 2011; 54: 2096–104.

Butson CR, Maks CB, McIntyre CC. Sources and effects of electrode impedance during deep brain stimulation. Clin Neurophysiol 2006; 117: 447–54.

Coenen VA, Allert N, Paus S, Kronenburger M, Urbach H, Madler B. Modulation of the cerebello-thalamo-cortical network in thalamic deep brain stimulation for tremor: a diffusion tensor imaging study. Neurosurgery 2014; 75: 657–69; discussion 69–70.

Cooper SE, Martin JH, Ghez C. Effects of inactivation of the anterior interpositus nucleus on the kinematic and dynamic control of multi-joint movement. J Neurophysiol 2000; 84: 1988–2000.

Deuschl G, Bain P, Brin M. Consensus statement of the Movement Disorder Society on Tremor. Ad Hoc Scientific Committee. Mov Disord 1998; 13 (Suppl 3): 2–23.

Deuschl G, Wenzelburger R, Raethjen J. Tremor. Curr Opin Neurol 2000; 13: 437–43.

Diener HC, Dichgans J, Bacher M, Gompf B. Quantification of postural sway in normals and patients with cerebellar diseases. Electroencephalogr Clin Neurophysiol 1984; 57: 134–42.

Elble RJ. Animal models of action tremor. Mov Disord 1998; 13 (Suppl 3): 35–9.

Elble RJ. Tremor: clinical features, pathophysiology, and treatment. Neurol Clin 2009; 27: 679–95, v–vi.

Fasano A, Herzog J, Raethjen J, Rose FE, Muthuraman M, Volkmann J, et al. Gait ataxia in essential tremor is differentially modulated by thalamic stimulation. Brain 2010; 133 (Pt 12): 3635–48.

Favilla CG, Ullman D, Wagle Shukla A, Foote KD, Jacobson CEt, Okun MS. Worsening essential tremor following deep brain stimulation: disease progression versus tolerance. Brain 2012; 135 (Pt 5): 1455–62.

Flament D, Hore J. Movement and electromyographic disorders associated with cerebellar dysmetria. J Neurophysiol 1986; 55: 1221–33.

Groppa S, Herzog J, Falk D, Riedel C, Deuschl G, Volkmann J. Physiological and anatomical decomposition of subthalamic neurostimulation effects in essential tremor. Brain 2014; 137 (Pt 1): 109–21.

Hallett M, Berardelli A, Matheson J, Rothwell J, Marsden CD. Physiological analysis of simple rapid movements in patients with cerebellar deficits. J Neurol Neurosurg Psychiatry 1991; 54: 124–33.

Hallett M, Dubinsky RM. Glucose metabolism in the brain of patients with essential tremor. J Neurol Sci 1993; 114: 45–8.

Hallett M, Massaquoi SG. Physiologic studies of dysmetria in patients with cerebellar deficits. Can J Neurol Sci 1993; 20 (Suppl 3): S83–92.

Hamel W, Schrader B, Weinert D, Herzog J, Volkmann J, Deuschl G, et al. MRI- and skull x-ray-based approaches to evaluate the position of deep brain stimulation electrode contacts—a technical note. Zentralbl Neurochir 2002; 63: 65–9.

Heiss WD, Habedank B, Klein JC, Herholz K, Wienhard K, Lenox M, et al. Metabolic rates in small brain nuclei determined by high-resolution PET. J Nucl Med 2004; 45: 1811–15.

Helmchen C, Hagenow A, Miesner J, Sprenger A, Rambold H, Wenzelburger R, et al. Eye movement abnormalities in essential tremor may indicate cerebellar dysfunction. Brain 2003; 126 (Pt 6): 1319–32.

Herzog J, Hamel W, Wenzelburger R, Potter M, Pinsker MO, Bartussek J, et al. Kinematic analysis of thalamic versus subthalamic neurostimulation in postural and intention tremor. Brain 2007; 130 (Pt 6): 1608–25.

Hilker R, Voges J, Weber T, Kracht LW, Roggendorf J, Baudrexel S, et al. STN-DBS activates the target area in Parkinson disease: an FDG-PET study. Neurology 2008; 71: 708–13.

Holsheimer J, Demeulemeester H, Nuttin B, de Sutter P. Identification of the target neuronal elements in electrical deep brain stimulation. Eur J Neurosci 2000; 12: 4573–7.

Ilg W, Golla H, Thier P, Giese MA. Specific influences of cerebellar dysfunctions on gait. Brain 2007; 130 (Pt 3): 786–98.

Imperato A, Nicoletti F, Diana M, Scapagnini U, Di Chiara G. Fastigial influences on postural tonus as studied by kainate lesions and by local infusion of GABAergic drugs in the rat. Brain Res 1984; 295: 51–63.

Ishii K, Senda M, Toyoma H, Oda K, Ishii K, Ishiwata K, et al. Brain function in bipedal gait: a PET study. Hum Brain Mapp 1995; 3: s321.

Itō M. The cerebellum and neural control. New York: Raven Press; 1984.

la Fougere C, Zwergal A, Rominger A, Forster S, Fesl G, Dieterich M, et al. Real versus imagined locomotion: a [18F]-FDG PET-fMRI comparison. Neuroimage 2010; 50: 1589–98.

Le Jeune F, Drapier D, Bourguignon A, Peron J, Mesbah H, Drapier S, et al. Subthalamic nucleus stimulation in Parkinson disease induces apathy: a PET study. Neurology 2009; 73: 1746–51.

Louis ED, Faust PL, Vonsattel JP, Honig LS, Rajput A, Robinson CA, et al. Neuropathological changes in essential tremor: 33 cases compared with 21 controls. Brain 2007; 130 (Pt 12): 3297–307.

Marple-Horvat DE, Criado JM. Rhythmic neuronal activity in the lateral cerebellum of the cat during visually guided stepping. J Physiol 1999; 518 (Pt 2): 595–603.

Marple-Horvat DE, Criado JM, Armstrong DM. Neuronal activity in the lateral cerebellum of the cat related to visual stimuli at rest, visually guided step modification, and saccadic eye movements. J Physiol 1998; 506 (Pt 2): 489–514.

Martin-Blanco A, Serra-Blasco M, Perez-Egea R, de Diego-Adelino J, Carceller-Sindreu M, Puigdemont D, et al. Immediate cerebral metabolic changes induced by discontinuation of deep brain stimulation of subcallosal cingulate gyrus in treatment-resistant depression. J Affect Disord 2015; 173: 159–62.

McNeal DR. Analysis of a model for excitation of myelinated nerve. IEEE Trans Biomed Eng 1976; 23: 329–37.

Nazzaro JM, Lyons KE, Pahwa R. Deep brain stimulation for essential tremor. Handb Clin Neurol 2013; 116: 155–66.

Otte A, Halsband U. Brain imaging tools in neurosciences. J Physiol Paris 2006; 99: 281–92.

Pahwa R, Lyons KE, Wilkinson SB, Simpson RK Jr, Ondo WG, Tarsy D, et al. Long-term evaluation of deep brain stimulation of the thalamus. J Neurosurg 2006; 104: 506–12.

Paxinos G, Mai JK. The human nervous system. . Amsterdam; Boston: Elsevier Academic Press; 2004.

Putzke JD, Wharen RE Jr, Obwegeser AA, Wszolek ZK, Lucas JA, Turk MF, et al. Thalamic deep brain stimulation for essential tremor: recommendations for long-term outcome analysis. Can J Neurol Sci 2004; 31: 333–42.

Reich MM, Steigerwald F, Sawalhe AD, Reese R, Gunalan K, Johannes S, et al. Short pulse width widens the therapeutic window of subthalamic neurostimulation. Ann Clin Transl Neurol 2015; 2: 427–32.

Romani M, Micalizzi A, Valente EM. Joubert syndrome: congenital cerebellar ataxia with the molar tooth. Lancet Neurol 2013; 12: 894–905.

Rühaak J, Derksen A, Heldmann S, Hallmann M, Meine H. Accurate CT-MR image registration for deep brain stimulation: a multi-observer evaluation study. Proc. SPIE 9413, Medical Imaging 2015: Image Processing, 941337, 2015.

Schwartz AB, Ebner TJ, Bloedel JR. Responses of interposed and dentate neurons to perturbations of the locomotor cycle. Exp Brain Res 1987; 67: 323–38.

Solomon DH, Barohn RJ, Bazan C, Grissom J. The thalamic ataxia syndrome. Neurology 1994; 44: 810–14.

Song IU, Ha SW, Yang YS, Chung YA. Differences in regional glucose metabolism of the brain measured with F-18-FDG-PET in patients with essential tremor according to their response to beta-blockers. Korean J Radiol 2015; 16: 967–72.

Sprague JM, Chambers WW. Regulation of posture in intact and decerebrate cat. I. Cerebellum, reticular formation, vestibular nuclei. J Neurophysiol 1953; 16: 451–63.

Velasco FC, Molina-Negro P, Bertrand C, Hardy J. Further definition of the subthalamic target for arrest of tremor. J Neurosurg 1972; 36: 184–91.

Wang J, Ma Y, Huang Z, Sun B, Guan Y, Zuo C. Modulation of metabolic brain function by bilateral subthalamic nucleus stimulation in the treatment of Parkinson's disease. J Neurol 2010; 257: 72–8.